

## Electronic evidence of asymmetry in the $\text{Si}(111)\sqrt{3}\times\sqrt{3}\text{-Ag}$ structure

Iwao Matsuda,<sup>1,\*</sup> Harumo Morikawa,<sup>1</sup> Canhua Liu,<sup>1</sup> Satoru Ohuchi,<sup>1</sup> Shuji Hasegawa,<sup>1</sup> Taichi Okuda,<sup>2</sup> Toyohiko Kinoshita,<sup>2</sup> Carlo Ottaviani,<sup>3</sup> Antonio Cricenti,<sup>3</sup> Marie D'angelo,<sup>4</sup> Patrick Soukiassian,<sup>4</sup> and Guy Le Lay<sup>5</sup>

<sup>1</sup>*Department of Physics, School of Science, the University of Tokyo, 7-3-1 Hongo, Bunkyo-ku, Tokyo 113-0033, Japan*

<sup>2</sup>*SRL-ISSP, the University of Tokyo, 5-1-5 Kashiwanoha, Kashiwa 277-8581, Japan*

<sup>3</sup>*Istituto di Struttura della Materia, Consiglio Nazionale delle Ricerche, Via Fosso del Cavaliere 100, 00133 Rome, Italy*

<sup>4</sup>*Commissariat a l'Energie Atomique, Saclay, DSM-DRECAM-SPCSI-SIMA, Bat. 462, 91191 Gif sur Yvette Cedex, France*

<sup>5</sup>*CRMC2-CNRS, Campus de Luminy, Case 913, 13288 Marseille Cedex 09, France*

(Received 2 April 2003; published 14 August 2003)

Our photoemission spectroscopy results clearly demonstrate that symmetry breakdown in atomic arrangement brings about a lift of degeneracy in electronic states, leading to settle a long-standing controversy on a surface superstructure. We provide unambiguous evidences that  $\text{Si}(111)\sqrt{3}\times\sqrt{3}\text{-Ag}$  has the inequivalent triangle structure (IET), excluding a long-lived honeycomb-chained triangle model. We also give critical experimental proof that the surface exhibits a disorder-order phase transition by cooling; the thermally fluctuating IET structure is frozen.

DOI: 10.1103/PhysRevB.68.085407

PACS number(s): 73.20.At, 79.60.Dp

Surface superstructures, which are formed on the first few atomic layers on clean or foreign-atom-adsorbed crystal surfaces, have provided interesting platforms for low-dimensional physics such as exotic phase transitions.<sup>1-5</sup> Comparing with low-dimensional bulk materials, phase transitions in surface superstructures have an experimental advantage that atomic positions, symmetries, and electronic structures at transitions can be directly probed with various surface science techniques. Such an example is a  $4\times 1$ -to- $8\times 2$ ' transition on an In/Si(111) surface upon cooling, observed by electron diffraction and scanning tunneling microscopy (STM).<sup>1</sup> The transition was found to be of metal-insulator type accompanying charge-density wave (CDW) formation through direct measurements of the Fermi surface and of the CDW gap by angle-resolved photoemission spectroscopy (ARPES). For other examples, temperature-induced transitions of  $2\times 1$ -to- $c(4\times 2)$  on a clean Si(001) surface<sup>2</sup> and  $\sqrt{3}\times\sqrt{3}$ -to- $3\times 3$  on a Sn/Ge(111) surface<sup>3,4</sup> have been widely interpreted in terms of an order-disorder phase transition; the high-temperature phases consist of time-averaged structures by thermal fluctuations, while the low-temperature (LT) phases are composed of frozen structures with periodic modulations in atomic positions. Since the photoemission process is much faster in time scale than thermal fluctuations, electronic studies by means of photoemission spectroscopy, again, played crucial roles in determining transition mechanisms.<sup>2-5</sup> Nonmetallic character at Fermi level ( $E_F$ ) for the Si(001) surface<sup>2</sup> and multicomponents in core-level photoemission for the Sn/Ge(111) surface<sup>3</sup> were not changed through the transitions, which were decisive keys to solve the nature of phase transitions.

In this paper, we show another example of electronic evidence for an asymmetric structure, which was believed to be a symmetric structure, and also evidence for an order-disorder phase transition, and provide a consistent view on a controversial surface structure. A  $\text{Si}(111)\sqrt{3}\times\sqrt{3}$  superstructure, induced by one monolayer (ML) Ag adsorption on a Si(111) crystal, has been historically the most important

prototype for the metal/semiconductor interface<sup>6-8</sup> and also recently an inevitable model to make interpretations for static and dynamic images of surface probe microscopies, i.e., STM and atomic force microscopy.<sup>8-14</sup> With these fundamental physical and nanotechnological importances, the surface is reinvestigated in detail by ARPES in the present research.

Its empty-state STM images are known to display a honeycomb-lattice pattern at room temperature (RT),<sup>9-11</sup> while hexagonal-lattice pattern at LT (62 K).<sup>14,15</sup> So two structural models have been proposed for the phases at RT and LT. They are called a "honeycomb-chained triangle" (HCT) model with a higher symmetry ( $p31m$  space group)<sup>10,11,16,17</sup> and an "inequivalent triangle" (IET) model with a lower symmetry ( $p3$  space group),<sup>14</sup> respectively. The models are schematically shown in Fig. 1(a). The HCT structure model is characterized by Ag trimers (denoted as tri-

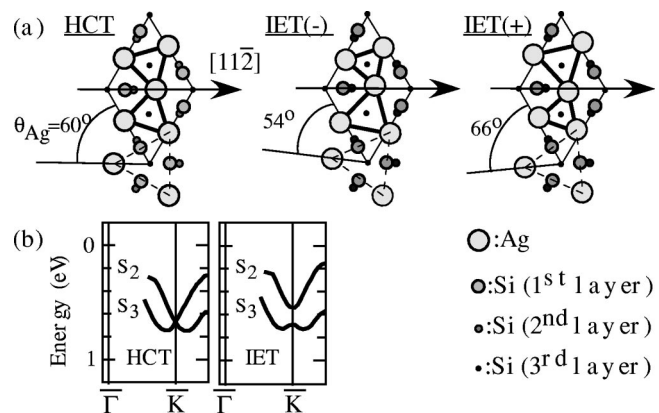


FIG. 1. (a) Schematic illustrations of the HCT and IET models for the  $\text{Si}(111)\sqrt{3}\times\sqrt{3}\text{-Ag}$  surface. Thin solid lines indicate the unit cell and thick ones represent Ag trimers. The triangles with thin broken lines and the angles ( $\theta_{\text{Ag}}$ 's) are drawn to show the differences between HCT, IET(-), and IET(+). (b) Schematic illustrations of the calculated band structure along  $[11\bar{2}]$  axis for the HCT and IET models (Ref. 14).

angles with solid thick lines in Fig. 1) arranged in a honeycomb lattice; these trimers are all equivalent to each other and their arrangement contains a mirror symmetry plane along the  $[11\bar{2}]$  axis.<sup>16,17</sup> In the IET model, the positions of three Ag atoms in each unit cell are slightly rotated in the same direction around the cell corner from those of the HCT structure. Since there are two rotation directions, the IET structure is classified into two domains IET(-) and IET(+), as shown in Fig. 1(a). As a consequence two inequivalent Ag triangles of different sizes are formed in an unit cell, and a mirror plane along  $[11\bar{2}]$  crystal axis in the HCT model disappears in the IET model, being a kind of (local) symmetry breakdown. While the recent first-principle calculations showed that the IET model is energetically more stable than the HCT,<sup>14</sup> the previous ARPES studies reported a surface band structure supporting the HCT model.<sup>18,19</sup> Moreover recent surface x-ray diffraction (SXRD) supported the HCT structure with a large thermal fluctuation at RT, which transforms into the IET structure below 150 K.<sup>16,20</sup> On the other hand, the recent theoretical simulations have suggested that the RT phase is not a static HCT structure but rather a thermally fluctuating structure between IET(-) and IET(+).<sup>12,13,21</sup> Then we are faced with fundamental questions. (1) In spite of the first-principle calculation telling that the HCT structure is not the most stable structure, does it really exist at RT? (2) What is the nature of long-range-order symmetry transition between the honeycomb and hexagonal lattice patterns in STM images? Is this a transition from the HCT to the IET structures with cooling? In the present work, these specific questions are solved in the light of a general principle of physics that symmetry breakdown in atomic arrangement causes a lift of degeneracy in electronic states. We have found that two surface-state bands for this surface superstructure, which should be degenerate at  $\bar{K}$  point for the HCT model,<sup>10,11,14</sup> are not actually degenerate both in its high- and low-temperature phases, in contradiction to the previous ARPES reports.<sup>18,19</sup> This is a direct evidence for that the RT phase, which has been believed to be the HCT structure<sup>10,11,16,17</sup> for twenty years,<sup>6-8</sup> is a time-averaged thermally fluctuating local IET structure.<sup>14</sup> We also found that a disorder-order type phase transition proceeds by cooling and the surface changes into the frozen IET structure at LT. Such a transformation naturally explains the honeycomb-to-hexagonal lattice patterns observed in STM images.<sup>9-11,14,15</sup>

The ARPES experiments were performed with unpolarized He  $I\alpha$  radiation and with linearly polarized synchrotron radiation (SR) at beamline (BL)-3.2R at ELLETRA, Italy, and also at BL-18A of KEK-Photon Factory, Japan. ARPES spectra were taken from  $\sim 90$  K up to RT. The temperature was measured by thermocouples fixed on the sample holder close to the sample. The spectra shown here were taken at 120 K, if not specified, and normalized by background intensities above  $E_F$ .<sup>22</sup> The  $E_F$  position was determined by fitting the Fermi edge measured on Ta foils holding Si crystals. An  $n$ -type (P-doped) Si(111) wafer (2–15  $\Omega$  cm) was cleaned *in situ* by direct current heating, up to 1250 °C. A Si(111) $\sqrt{3} \times \sqrt{3}$ -Ag surface was prepared by evaporating  $\sim 1.2$  ML of

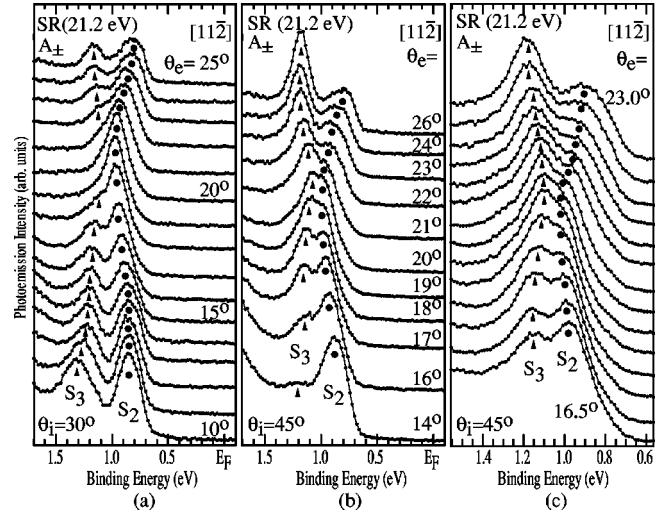


FIG. 2. Normalized ARPES spectra for the Si(111) $\sqrt{3} \times \sqrt{3}$ -Ag surface taken along the surface Brillouin zone line  $\bar{\Gamma}-\bar{K}$  ( $[11\bar{2}]$  axis), with SR at 120 K in the  $A_{\pm}$  geometry (see the text). The photon energy used is 21.22 eV and the photon incident angles ( $\theta_i$ 's) are (a) 30°, (b) 45°, and (c) 45°.

Ag on the Si(111) $7 \times 7$  clean surface at  $\sim 520$  °C, followed by further annealing at 520–540 °C and  $\sim 600$  °C.<sup>23</sup> The quality of the surface was ascertained by a sharp  $\sqrt{3} \times \sqrt{3}$  electron diffraction pattern, fine structures of the Si  $2p$  spectra,<sup>23</sup> and strong surface state signals of the ARPES spectra.<sup>18,23-26</sup> In order to investigate the symmetry properties of the surface states along  $[11\bar{2}]$  axis, we adopted two different measurement geometries denoted as  $A_+$  and  $A_{\pm}$ .<sup>18,22</sup> In brief, photoelectrons only from even-symmetry initial states are detected in the  $A_+$  geometry, while initial states of both even and odd symmetries are probed in the  $A_{\pm}$  geometry. Linear polarization for the data shown below is confirmed to be better than 90%, satisfying the experimental condition.

Figure 2 shows the ARPES spectra measured with photon energy ( $h\nu$ ) of 21.22 eV (SR), scanned along the  $\bar{\Gamma}-\bar{K}$  surface Brillouin zone (SBZ) line ( $[11\bar{2}]$  axis), in the  $A_{\pm}$  geometry, (a) at an incident angle of photon ( $\theta_i$ ) = 30°, (b) at  $\theta_i = 45^\circ$ , and (c) at  $\theta_i = 45^\circ$  with fine scans (in 0.5° step) near  $\bar{K}$  point [corresponding to an emission angle ( $\theta_e$ ) of  $\sim 20^\circ$ ]. The scan direction of  $[11\bar{2}]$  axis was determined by low or reflection-high-energy electron diffraction with a precision of  $\sim \pm 0.1^\circ$ . In these spectra, two prominent peaks, denoted by  $S_2$  and  $S_3$ , are observed at a binding energy ( $E_B$ )  $\sim 1$  eV, which are attributed to the surface states.<sup>18,19,24,25</sup>

The spectral appearances of  $S_2$  and  $S_3$  states are different between the measurement conditions due to the photoemission matrix element.<sup>18,27</sup> Such a distinction enables us to trace the dispersions of  $S_2$  and  $S_3$  with  $\theta_e$  individually. The  $S_2$  and  $S_3$  states disperse and approach each other at  $\theta_e \sim 20^\circ$  ( $\bar{K}$  point). However, they do not degenerate or cross each other. Figure 3 shows gray-scale band dispersion diagrams constructed from the spectra in Fig. 2. The intensities of the spectral features are approximately represented by the

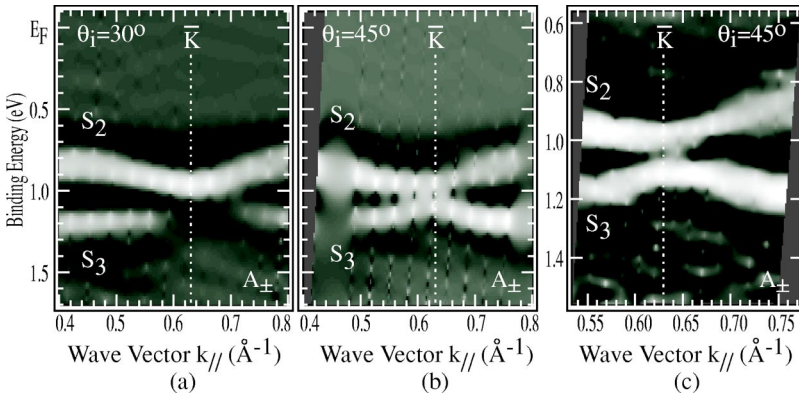


FIG. 3. Gray-scale diagrams of the surface-state band dispersions along  $\bar{\Gamma}-\bar{K}$  ( $[11\bar{2}]$  axis), constructed from the ARPES scans in Figs. 2(a), 2(b), and 2(c), respectively.

brightness in gray-scale by taking the second derivatives of the original ARPES spectra.<sup>22</sup> As can be seen, the  $S_2$  and  $S_3$  states energetically come closer near  $\bar{K}$  point, but keep an energy gap between them. Through our ARPES experiments at different chambers and spectrometers, the gap was determined to be  $0.22 \pm 0.07$  eV. The two states never degenerate at the  $\bar{K}$  point. As shown in Fig. 1, the recent first-principles calculations have reported that, at the  $\bar{K}$  point,  $S_2$  and  $S_3$  should be degenerate for the HCT model, while they are not degenerate, having an energy gap of 0.15 eV for the IET model.<sup>14</sup> This value is very close to our experimental result. This firmly supports that the surface has the IET structure at 120 K, not the HCT. No previous works of ARPES studies on the electronic structure of this surface<sup>18,19,23-25</sup> reported this band splitting.

Contrary to our results, the previous ARPES studies<sup>18</sup> under the same conditions showed that the  $S_2$  and  $S_3$  states are degenerate at  $\bar{K}$  point, where only a broad single peak was observed. Figure 2(b) in the present study shows that the  $S_2$  and  $S_3$  peaks are enhanced below and above  $\theta_e = 20^\circ$  ( $\bar{K}$ ), respectively. Thus, we can infer that the broad peak observed in the previous report<sup>18</sup> was composed of the unresolved  $S_2$  and  $S_3$  components, and that the spectral signature of these components seemingly behaved as if a single state was dispersing to higher  $E_B$  with emission angles. The clear separation between the  $S_2$  and  $S_3$  components in our ARPES spectra stems from a recently proposed procedure for well-controlled sample preparation,<sup>23</sup> LT measurements to reduce phonon broadening, and fine scans with smaller angle steps.

It is confirmed by experiments and theories that  $\text{Si}(111)\sqrt{3} \times \sqrt{3}\text{-Ag}$  possesses another surface state  $S_1$  near  $E_F$ .<sup>14,18,19,23,25</sup> Yet, the calculation shows that the HCT and IET models have different  $E_B$ 's for the  $S_1$  state.<sup>14</sup> However, due to limited accuracy in determining the  $E_F$  position in the first-principles calculation<sup>14</sup> as well as experimental difficulty in determining  $E_B$  of  $S_1$ ,<sup>18,23</sup> the state can never be the proper criterion. In this research, we have obtained the consistency of  $S_1$  with the previous ARPES studies<sup>18,19,23,25</sup> and confirmed that the behavior of this state does not alter the  $S_2$  and  $S_3$  results.

Next let us discuss the symmetry properties of the  $S_2$  and  $S_3$  wave functions. In the previous ARPES study,<sup>18</sup> it was reported that the  $S_3$  state had odd symmetry with respect to the mirror plane along  $[11\bar{2}]$  axis, which supported the HCT

model,<sup>10</sup> and that the state should not be observed in SR-ARPES measurements in the  $A_+$  geometry. Figure 4 shows ARPES spectra taken along  $[11\bar{2}]$  ( $\bar{\Gamma}-\bar{K}$  direction) in the  $A_+$  geometry at  $h\nu = 21.22$  eV (SR). The two states  $S_2$  and  $S_3$  are clearly observed, implying that  $S_3$  has no odd symmetry with respect to  $[11\bar{2}]$  axis. While a complete argument of the missing symmetry elements requires a proper calculation on photoemission matrix elements with detail characterizations of SR linearity, no defined mirror symmetry plane may be derived along  $[11\bar{2}]$  axis for both the  $S_2$  and  $S_3$  wave functions. This is consistent with the ARPES results of the IET structure given above.

Now, we can be sure that the electronic structure, derived from the ARPES measured at 120 K, is consistent with the lower-symmetry IET structure, rather than the higher-symmetry HCT model. Next we discuss the observed transition in STM images by cooling, from a honeycomb lattice

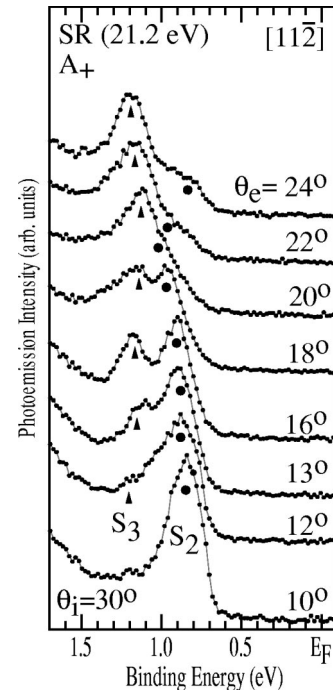


FIG. 4. Normalized ARPES spectra taken along  $\bar{\Gamma}-\bar{K}$  ( $[11\bar{2}]$  axis) at 120 K in the  $A_+$  geometry (see text) with SR of  $h\nu = 21.22$  eV and  $\theta_i = 30^\circ$ .



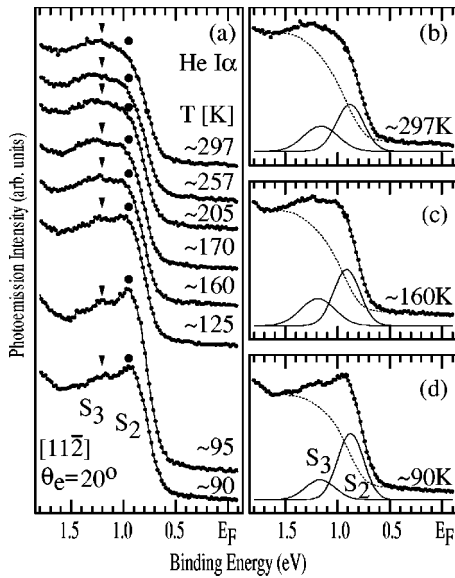


FIG. 5. (a) ARPES spectra at the  $\bar{K}$  point measured at various temperatures, taken with He  $I\alpha$  radiation at  $\theta_i = 40^\circ$  and  $\theta_e = 20^\circ$ . (b)–(d) Decompositions of the spectra at  $\sim 297$  K (b),  $\sim 160$  K (c), and  $\sim 90$  K (d); the raw data and fitting curves are shown as dots and lines, respectively.

pattern at RT (Refs. 9,10,14) to a hexagonal one at LT.<sup>14,15</sup> Since, according to the STM image simulations,<sup>11,14</sup> the honeycomb and hexagonal lattice patterns are consistent with the HCT and IET models, respectively, a straightforward interpretation is that the observed change in STM images is a transition from the HCT to IET by cooling, being an order-order transition. If it is the case, the  $S_2$  and  $S_3$  states would change at  $\bar{K}$  point by cooling; the two states would be degenerate at RT and split at LT. Then, we measured spectra just at  $\bar{K}$  point, as a function of temperature.

Figure 5(a) shows a series of ARPES spectra at the  $\bar{K}$  point ( $\theta_e = 20^\circ$ ) taken at various temperatures ranging from  $\sim 90$  to  $\sim 297$  K with He  $I\alpha$  radiation at  $\theta_i = 40^\circ$ . At 90 K, the  $S_2$  and  $S_3$  peaks are clearly distinguished as in Figs. 2–4. With increasing temperatures, the spectral signature of

the two peaks energetically broadens. However, one can be fairly certain from the raw spectra that the two peaks persist at any temperature. To analyze this point in detail, we decomposed the spectra at each temperature, using two Gaussian peaks and an integrating background,<sup>3</sup> as shown in Figs. 5(b)–5(d). The full widths at half maximum of the Gaussian peaks are 0.29 ( $S_2$ ) and 0.34 eV ( $S_3$ ) at 90 K in (d); they are slightly broadened in (b) and (c). It is then obvious that there are always two components at all temperatures; their binding energies do not change with temperature. The slight change of the relative intensities of two components with temperature may be owing to the background subtraction or has also been reported for typical order-disorder transition systems.<sup>2,3</sup> Thus, there is no change in electronic structure.

A presence of a gap at the  $\bar{K}$  point at every observed temperature unambiguously indicates an existence of no mirror symmetry plane along  $[11\bar{2}]$  crystal axis at  $\sim 90$ –297 K. This result favors a transition of order-disorder type for the transition rather than structural one. It is now experimentally confirmed that the AFM/STM images taken at RT are time-averaged images of the thermal fluctuations. The previous calculation of the order-disorder type predicted a transition temperature below RT and higher probability of IET than that of HCT even at RT,<sup>12</sup> being consistent with the previous STM studies<sup>8–14</sup> and the present ARPES results. The theoretical approach also proposed several possible metastable structures that are much stable than the HCT one.<sup>12</sup> Since the result of Fig. 5 only teaches local symmetry of the surface, it leaves rooms for existence of such metastable structures or a certain change in the IET structure, such as  $\theta_{Ag} < 6^\circ$ , with temperature. This seemingly makes consensus with the SXRD results<sup>20</sup> and suggests that Si(111) $\sqrt{3} \times \sqrt{3}$ -Ag could be an interesting playground to study order-disorder phase transition with fluctuation among continuous states, which might belong to a different class from the multistate Potts model.

Mr. M. Konishi, Ms. A. Harasawa, and Dr. S. Fontana are gratefully acknowledged for their help during the experiments. This work has been supported by Grants-In-Aid from Japanese Society for the Promotion of Science.

\*Electronic address: matsuda@surface.phys.s.u-tokyo.ac.jp

<sup>1</sup>H.W. Yeom, S. Takeda, E. Rotenberg, I. Matsuda, K. Horikoshi, J. Schaefer, C.M. Lee, S.D. Kevan, T. Ohta, T. Nagao, and S. Hasegawa, Phys. Rev. Lett. **82**, 4898 (1999).

<sup>2</sup>Y. Enta, S. Suzuki, and S. Kono, Phys. Rev. Lett. **65**, 2704 (1990).

<sup>3</sup>R.I.G. Uhrberg and T. Balasubramanian, Phys. Rev. Lett. **81**, 2108 (1998).

<sup>4</sup>J. Avila, A. Mascaraque, E.G. Michel, M.C. Asensio, G. LeLay, J. Ortega, R. Perez, and F. Flores, Phys. Rev. Lett. **82**, 442 (1999).

<sup>5</sup>L. Petersen, Ismail, and E.W. Plummer, Prog. Surf. Sci. **71**, 1 (2002).

<sup>6</sup>G. Le Lay, V.Yu. Aristov, L. Seehofer, T. Buslaps, R.L. Johnson, M. Gothelid, M. Hammer, U.O. Karlsson, S.A. Flodström, R. Feidenhans'l, M. Nielsen, E. Findeisen, and R.I.G. Uhrberg, Surf. Sci. **307-309**, 280 (1994).

<sup>7</sup>S. Hasegawa, X. Tong, S. Takeda, N. Sato, and T. Nagao, Prog.

Surf. Sci. **60**, 89 (1999).

<sup>8</sup>J. Nogami, Surf. Rev. Lett. **1**, 395 (1994).

<sup>9</sup>K.J. Wan, X.F. Lin, and J. Nogami, Phys. Rev. B **45**, 9509 (1992).

<sup>10</sup>Y.G. Ding, C.T. Chan, and K.M. Ho, Phys. Rev. Lett. **67**, 1454 (1991); **69**, 2452 (1992).

<sup>11</sup>S. Watanabe, M. Aono, and M. Tsukada, Phys. Rev. B **44**, 8330 (1991).

<sup>12</sup>Y. Nakamura, Y. Kondo, J. Nakamura, and S. Watanabe, Phys. Rev. Lett. **87**, 156102 (2001); Surf. Sci. **493**, 206 (2001).

<sup>13</sup>N. Sasaki, S. Watanabe, and M. Tsukada, Phys. Rev. Lett. **88**, 046106 (2002); Surf. Sci. **493**, 188 (2001).

<sup>14</sup>H. Aizawa, M. Tsukada, N. Sato, and S. Hasegawa, Surf. Sci. **429**, L509 (1999).

<sup>15</sup>N. Sato, T. Nagao, and S. Hasegawa, Surf. Sci. **442**, 65 (1999).

<sup>16</sup>T. Takahashi and S. Nakatani, Surf. Sci. **282**, 17 (1993).

<sup>17</sup>M. Katayama, R.S. Williams, M. Kato, E. Nomura, and M. Aono,

- Phys. Rev. Lett. **66**, 2762 (1991).
- <sup>18</sup>L.S.O. Johansson, E. Landemark, C.J. Karlsson, and R.I.G. Uhrberg, Phys. Rev. Lett. **63**, 2092 (1989); **69**, 2451 (1992).
- <sup>19</sup>H.M. Zhang, K. Sakamoto, and R.I.G. Uhrberg, Phys. Rev. B **64**, 245421 (2001).
- <sup>20</sup>H. Tajiri, K. Sumitani, S. Nakatani, A. Nojima, T. Takahashi, K. Akimoto, H. Sugiyama, X. Zhang, and H. Kawata (unpublished).
- <sup>21</sup>K. Kakitani, A. Yoshimori, H. Aizawa, and M. Tsukada, Surf. Sci. **493**, 200 (2001).
- <sup>22</sup>I. Matsuda, H.W. Yeom, K. Tono, and T. Ohta, Phys. Rev. B **59**, 15 784 (1999).
- <sup>23</sup>R.I.G. Uhrberg, H.M. Zhang, T. Balasubramanian, E. Landemark, and H.W. Yeom, Phys. Rev. B **65**, 081305 (2002).
- <sup>24</sup>T. Yokotsuka, S. Kono, S. Suzuki, and T. Sagawa, Surf. Sci. **127**, 35 (1983).
- <sup>25</sup>X. Tong, S. Ohuchi, N. Sato, T. Tanikawa, T. Nagao, I. Matsuda, Y. Aoyagi, and S. Hasegawa, Phys. Rev. B **64**, 205316 (2001).
- <sup>26</sup>X. Tong, C.S. Jiang, and S. Hasegawa, Phys. Rev. B **57**, 9015 (1998).
- <sup>27</sup>H.-J. Neff, I. Matsuda, M. Hengsberger, F. Baumberger, T. Greber, and J. Osterwalder, Phys. Rev. B **64**, 235415 (2001).